JOURNAL OF MATERIALS SCIENCE 26 (1991) 1793–1798

Temperature dependence of the elastic moduli and damping for polycrystalline LiF–22% CaF_2 eutectic salt

A. WOLFENDEN, G. LASTRAPES, M. B. DUGGAN
Texas A & M University, Mechanical Engineering Department and Advanced Materials Laboratory, College Station, Texas 77843-3123, USA

S. V. RAJ,
NASA Lewis Research Center, MS 49-1, 21000 Brookpark Road, Cleveland, Ohio 44135, USA

The Young's and shear moduli and damping were measured for as-cast polycrystalline LiF–22 (mol%) CaF_2 eutectic specimens as a function of temperature using the piezoelectric ultrasonic composite oscillator technique (PUCOT). The shear modulus decreased with increasing temperature from about 40 GPa at 295 K to about 30 GPa at 1000 K, while the Young's modulus decreased from about 115 GPa at 295 K to about 35 GPa at 900 K. These values are compared with those derived from the rule of mixtures using elastic moduli data for LiF and CaF_2 single crystals. It is shown that, while the shear modulus data agree reasonably well with the predicted trend, there is a large discrepancy between the theoretical calculations and the Young's modulus values, where this disagreement increases with increasing temperature. The reason for this discrepancy is unclear but several possibilities are examined and discussed. The effective activation energy for damping was determined to be about 0.21 eV/atom which was found to be in reasonable agreement with the activation energy for migration of anion vacancies in the CaF_2 phase.

1. Introduction

Advanced solar dynamic systems, containing thermal energy storage units, are currently being designed to provide a continuous supply of electrical power for orbiting spacecraft. The basic function of a thermal energy storage (TES) unit is to store heat energy collected during the sunlight portion of an orbit and to release it when the vehicle is in eclipse with this energy storage and release being attained by a thaw–freeze cycle of a TES material. The attractive thermophysical properties of fluoride salts [1, 2] make them potential candidates for use as thermal energy storage materials in advanced solar dynamic systems. In particular, the LiF–CaF_2 eutectic mixture containing about 21 (mol %) CaF_2 [3] is under consideration for use as the thermal energy storage material for space-based solar dynamic systems [4].

A major problem that arises with the use of fluoride salts as energy storage materials is the high volume expansion ($\approx 30\%$) that they undergo on melting. This can lead to a stress build-up on the walls of the container when pockets of molten material are entrapped between the containment vessel and the unmelted salt [5, 6]. Under such conditions, it is conceivable that localized distortion or rupture of the containment vessel can occur if the volume expansion of the liquid is not accommodated by the deformation or fracture of the unmelted salt.

Clearly, in order to design a suitable salt containment unit for solar dynamic systems, which must maintain its structural integrity for tens of years, it is desirable that the mechanical properties of the LiF–CaF_2 eutectic material be characterized as a function of temperature, strain rate and microstructure. The strength characteristics of this salt have been reported elsewhere [5–7], and the present paper presents the results of dynamic elastic moduli and damping measurements conducted on the eutectic. The elastic moduli data are expected to provide useful information in evaluating the thermal stresses generated within the salt, which are likely to influence the magnitude of the stresses acting on the containment wall.

2. Experimental procedure

The material used in this investigation was produced from Cerac, Inc. in the form of a randomly cast ingot of a slightly CaF_2-rich hypereutectic composition (Table I). The LiF–CaF_2 shows no measurable terminal solid solution region [3] so that the eutectic salt is essentially a mixture of pure LiF and CaF_2 with the volume fraction of the latter being about 40% (Table I). Microstructural observations of the as-cast material showed large variations in the microstructure near the grain boundaries as illustrated by the typical

0022–2461/91 $03.00 + .12

TABLE I Chemical composition of the as-cast material.

Phase	mol(%)	vol(%)	wt(%)
CaF_2	21.9	41.0	45.8
LiF	78.1	59.0	54.2

Impurities (wt%): Al: <0.001%; Cu: <0.001%; Fe: 0.005%; Mg: 0.005%; Si: 0.001%.

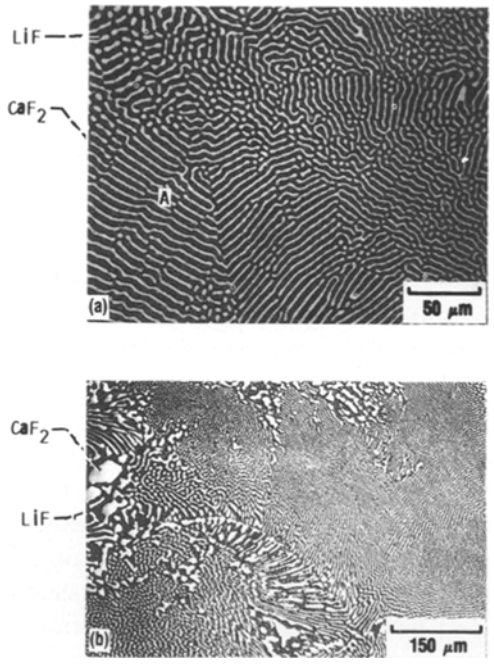

Figure 1 Representative (a) optical and (b) back scattered electron micrographs of undeformed as-cast LiF–22% CaF_2 material after etching. (a) The eutectic lamellae are fairly intact near the grain boundaries. (b) The eutectic microstructure has broken down near the grain boundaries.

optical and back scattered electron (BSE) micrographs shown in Fig. 1a and b, respectively. While the lamellar microstructure is well defined within the grains and fairly intact at most of the grain boundaries in Fig. 1a, this is not the case in the regions shown in Fig. 1b. In the latter instance, the lamellar structure in the vicinity of the grain boundary is either very coarse or non-existent, so that two neighbouring grains are separated by a broad transition region consisting of globules of CaF_2 in a matrix of LiF. The inter-lamellar spacing, λ, was reasonably uniform within each grain although the lamellae showed evidence of kinking and growth faults in some regions (e.g. grain A in Fig. 1a). The frequency distribution plots for the nodule or grain size, d, and λ were fairly wide, where both these quantities were measured by the linear intercept technique [5, 6]. The modes of the distribution functions for grain size and inter-lamellar spacing occurred at $d_{mode} \approx 350$ μm and $\lambda_{mode} \approx 2.3$ μm, respectively, with the mean values occurring at $d_{mean} = 645$ μm and $\lambda_{mean} \approx 2.8$ μm, respectively.

Dynamic Young's modulus, E, and damping or internal friction, Q^{-1}, measurements were conducted simultaneously on rectangular specimens of approximate dimensions $40 \times 3 \times 3$ mm^3 which were cut from random locations in the casting using a diamond saw with water as a lubricant. Cylindrical specimens approximately 50 mm long and 6.4 mm in diameter were core drilled parallel to the ingot thickness, and these were used in the dynamic shear modulus, G, measurements. The ends of all specimens were polished with 600 emery paper in order to ensure proper contact with the piezoelectric transducer.

The measurements of E and G were made with the piezoelectric ultrasonic composite oscillator technique (PUCOT) [8–12] operating at frequencies of 150 and 80 kHz, respectively, and at temperatures between 295 and 1020 K. However, in one instance, Young's modulus measurements were conducted at 638 K over a 24 h period on a core drilled specimen using a resonating frequency of 80 kHz in order to confirm the data obtained on the randomly cut specimens. Allowances were made for changes in length and density of the specimen with temperature by using appropriate values of the coefficient of thermal expansion (CTE) estimated from CTE data for CaF_2 and LiF [13]. The reproducibilities of the E and G measurements were approximately ± 2.3 and ± 5.6%, respectively.

After measurements with the PUCOT, representative specimens were ground and polished sufficiently to expose the central regions, which were then examined by optical microscopy. These observations revealed that the total volume fraction of pores was less than 2%, and that there were at least 7 to 10 grains across the thickness section in these specimens. However, there were significant differences in the microstructures of the randomly cut and core-drilled specimens. The randomly cut specimens used for determining E consisted essentially of equiaxed grains (Fig. 1a), while the core-drilled samples used for measuring G had a significantly larger number of columnar grains, which extended between 1/3 to 1/2 of the specimen length with the eutectic lamellae being almost perpendicular to the growth axes of these grains in most instances.

3. Results and discussion

3.1. Temperature dependence of the elastic moduli

The measured values of E, G and Q^{-1} are tabulated in Table II as a function of the absolute temperature, T. Fig. 2 compares the temperature dependence of the experimental values of the shear modulus with the upper and lower bounds predicted by the rule of mixtures (ROM) calculated from

$$G_{ROM} = V_f G_f + V_m G_m \quad (1)$$

where G_{ROM} is the shear modulus, V_f and V_m are the volume fractions of CaF_2 and LiF, respectively, and G_f and G_m are the estimated shear moduli of polycrystalline CaF_2 and LiF, respectively (Appendix). The procedure employed in deriving the upper and lower bounds predicted by the rule of mixtures approach based on the moduli of the individual phases is outlined in the Appendix. The experimental values of G decrease linearly with increasing temperature from $G \approx 43$ GPa at $T \approx 300$ K to $G \approx 27$ GPa at $T \approx 1020$ K. It is evident from Fig. 2 that the experi-

TABLE II Measured values of Young's and shear moduli and damping for polycrystalline LiF–22% CaF_2.

T (K)	E^a (GPa)	G^b (GPa)	Q^{-1}
295	115.8	42.6	3.9×10^{-3}
450	97.8	—	8.4×10^{-4}
450	95.3	—	1.4×10^{-3}
495	—	40.5	—
515	85.3	—	1.4×10^{-3}
675	—	38.3	—
680	63.0	—	7.9×10^{-3}
745	58.6	—	1.0×10^{-2}
785	—	30.7	—
879	—	25.8	—
900	35.5	—	1.4×10^{-2}
940	—	24.6	—
1005	—	30.1	—
1005	—	30.4	—
1013	—	30.7	—
1019	—	26.3	—
1019	—	27.8	—

[a] The Young's moduli were determined on specimens cut randomly from the ingot using a resonance frequency of 150 kHz.
[b] The shear moduli measurements were conducted on core-drilled specimens with their axes parallel to the thickness of the ingot using a resonance frequency of 80 kHz.

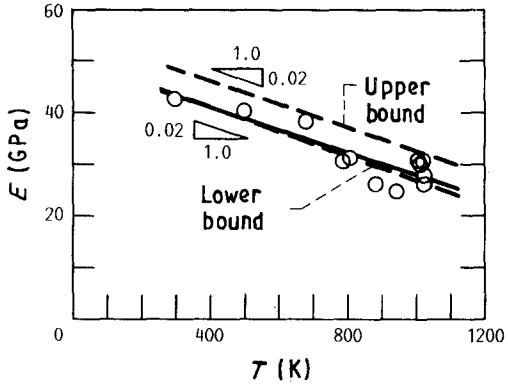

Figure 2 Comparison of the experimental values (○) of shear modulus for LiF–22% CaF_2 with the upper and lower bounds predicted by the rule of mixtures (---).

mental data are scattered about a linear regression line given by the relation

$$G = 49.6 - 0.0218\,T(\text{GPa}) \quad (2)$$

where the correlation coefficient was found to be 0.88. Fig. 2 also demonstrates that the lower bound predicted by the rule of mixtures is in good agreement with the experimental data.

Fig. 3 shows the temperature dependence of the Young's modulus where it is seen that E decreases linearly with increasing temperature from $E \approx 115$ GPa at $T \approx 300$ K to $E \approx 35$ GPa at $T = 900$ K. The broken lines shown in Fig. 3 represent the upper and lower values of Young's modulus calculated from the rule of mixtures using the procedure outlined in the Appendix. A single datum obtained at 638 K on a core-drilled specimen is also shown. It is apparent from Fig. 3 that the predicted and the experimental

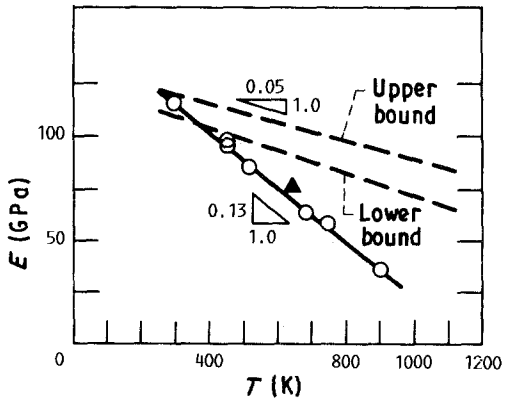

Figure 3 Comparison of the experimental values (○) of Young's modulus (150 Hz) for randomly-sectional LiF–22% CaF_2 specimens with the upper and lower bounds predicted by the rule of mixtures (---). ▲ represents the Young's modulus for a core drilled specimen (80 Hz).

values of Young's modulus are not in agreement with each other above 400 K, and that this discrepancy increases with increasing temperature. A regression line through the experimental data gave

$$E = 155.2 - 0.133\,T(\text{GPa}) \quad (3)$$

with a correlation coefficient of 0.998.

This disagreement between the experimental and the theoretical data for E cannot be attributed to any porosity present in the material for three reasons. First, the PUCOT is relatively insensitive to microstructural defects of the order of a pore size since the wavelengths of the standing strain and displacement waves are twice the length of the specimen [12]. Second, the temperature dependence of the shear modulus does not show a similar disagreement with the ROM results as the Young's modulus data (Fig. 2). Third, an estimate of the decrease in the Young's modulus due to porosity calculated from [14]

$$E = E_0(1 - 1.9P + 0.9P^2) \quad (4)$$

where E_0 is the Young's modulus of the dense material and P is the volume fraction of closed pores, suggested that E is only about 5% of E_0 for the experimental value of $P \approx 0.02$.

It was reported in an early investigation on aluminium, copper and nickel that residual strains and excess dislocations produced by cold working these metals by 20% resulted in lowering the dynamic Young's modulus by about 1 to 3% [15, 16]. As shown in Fig. 3, this is not the case for the present set of data where the discrepancy between the predicted and the experimental values of E increases with increasing temperature so that they differ from each other by more than 55% at 900 K. Thus, residual strains present within the ingot cannot account for the present observations.

It may be argued that the inconsistency arising from the good agreement between the shear modulus data and those expected from the ROM results in one case (Fig. 2), and the discrepancy between the measured and the predicted values of Young's modulus on the other (Fig. 3), is due to the differences in the microstructure between the two sets of specimens described

in Section 2. Table III shows the values of E and Q^{-1} obtained on a core-drilled specimen tested at 638 K over a 24 h period. It is evident from Table III that there is no significant change over a 24 h period in the values of E and Q^{-1} which are about 75 GPa and 5 $\times 10^{-3}$, respectively. These observations confirm that residual strains cannot account for the results shown in Fig. 3. Furthermore, the agreement in the data shown in Fig. 3 for the core-drilled specimen and those with a random microstructure suggests that the elastic moduli measurements reported in this paper were not influenced significantly by the microstructure or resonance frequency (in the kHz range). Therefore, it must be concluded that the rule of mixtures does not apply to the Young's modulus data.

Assuming a Poisson's ratio, ν, of about 0.3, the measured values of G were converted to E using the istropic relation

$$E = 2(1 + \nu)G \quad (5)$$

A comparison of the values of E determined from Equation 5 with those measured directly (Fig. 3) confirmed that the two sets of results were not in agreement with each other. While it is possible that the salt may be anisotropic due to the presence of a solidification texture, X-ray diffraction peaks of the CaF_2 and LiF phases taken from three mutually perpendicular sections did not show any evidence of significant texture in the material. Due to the large grain size, which did not permit the incident X-ray beam to sample a large enough number of grains for statistical accuracy, no attempt was made to determine the pole figure for this material.

3.2. Activation energy for damping

Seven measurements of Q^{-1} conducted in the longitudinal wave mode yielded the data shown in Table II and Fig. 4. Apart from one outlying point obtained at room temperature, the results clearly indicate that the temperature dependence of damping is of the form

$$Q^{-1} = Q^{-1}(0)\exp(-\Delta H/kT) \quad (6)$$

where $Q^{-1}(0)$ is a reference value of damping, ΔH is the effective activation energy controlling the level of damping, and k is Boltzmann's constant. A linear regression fit to the data shown in Fig. 4 for $T > 300$ K gave values of $Q^{-1}(0) \approx 0.25$ and $\Delta H \approx 0.21 \pm 0.02$ eV/atom (i.e. 20.6 ± 2.3 kJ mol^{-1}) with a coefficient of correlation of about 0.98. In attempting to assign some physical significance to this value of the effective activation energy, it was necessary to compare it with the compiled data on experimental and theoretical activation energies for the formation and migration of several types of defects in CaF_2 [17–26] and LiF [27, 28] (Table IV). An examination of Table IV suggests that the present value of 0.21 eV/atom is in reasonable agreement with the values for anion vacancy migration in CaF_2 [25]. Thus, the temperature dependence of damping in LiF–22% CaF_2 appears to be related to the migration of anion vacancies in the CaF_2 phase of the eutectic material.

TABLE III Values of Young's modulus and damping at 638 K as a function of time for a resonant frequency of 80 kHz.

Time (h)	E (GPa)	Q^{-1}
0	74.4	4.8×10^{-3}
0.3	74.4	5.3×10^{-3}
22.7	75.1	4.8×10^{-3}

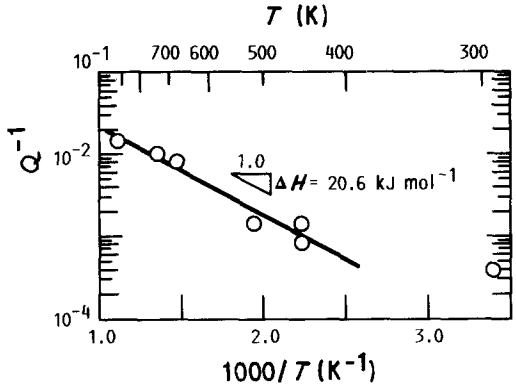

Figure 4 Variation of damping with the reciprocal of the absolute temperature for LiF-22% CaF_2.

TABLE IV Experimental and theoretical activation energies for several processes in CaF_2 and LiF.

Process	CaF_2 (eV/atom)	LiF (eV/atom)
Anion		
Formation energy of:		
(a) Frenkel pair	2.8 [17]	
	2.20–2.64 [18]	—
	2.20–3.1 [19]	
	2.70 [20]	
	2.70[a] [21, 22]	
(b) Schottky pair	—	2.17[a] [27]
Migration energy:		—
(a) interstitial	1.64 [17]	
(b) vacancy	0.52–0.88 [17]	
	0.81–1.02 [18]	
	0.65–1.20 [20]	
	0.36 [23]	
	0.54 [24]	
	0.17 [25]	
Cation		
Formation energy:		
(a) Frenkel pair	7.10[a] [22]	—
(b) Schottky trio	5.80[a] [22]	—
Migration energy of a vacancy	0.9–2.1[b] [19]	0.66[b] [28]
Associated energy of a dislocation-Frenkel pair	0.50[a] [26]	—

[a] Theoretical estimates.
[b] Estimated from the experimental data.

4. Summary and conclusions

The conclusions are as follows.

(1) Measurements of the Young's and the shear moduli for the LiF–22% CaF_2 eutectic as a function of the absolute temperature showed that these

elastic moduli decreased linearly with increasing temperature.

(2) The shear modulus data were in good agreement with the lower bound predicted by the rule of mixtures but a similar comparison with the experimentally determined values of Young's modulus was unsatisfactory.

(3) The effective activation energy for damping was 0.21 eV/atom and this value was found to be in reasonable agreement with published values for the migration of anion vacancies in the CaF_2 phase.

Acknowledgements

One of us (SVR) thanks the Advanced Solar Dynamics Branch of the Lewis Research Center for financial support through Cooperative Agreement NCC 3-72 with Cleveland State University. Another (AW) thanks the Summer Faculty Research Program, NASA Lewis Research Center and the American Society for Engineering Education for the award of a fellowship.

Appendix

A1 Equations used for estimating the polycrystalline elastic moduli from cubic single crystal data

Several equations have been proposed for estimating the elastic moduli of an isotropic polycrystalline material using cubic single crystal data on elastic stiffness, c_{ij}, or elastic compliance, s_{ij}, where $i = 1$ or 4 and $j = 1$, 2 or 4 [29]. The two most commonly used expressions are the Voigt and the Reuss models, respectively. The Voigt model, which is valid for the situation where the grain boundaries are parallel to each other so that the strain is uniform in all the grains, predicts that the shear modulus, G_V, and the bulk modulus, B_V, are given by

$$G_V = (c_{11} - c_{12} + 3c_{44})/5 \quad \text{(A1)}$$

and

$$B_V = (c_{11} + 2c_{12})/3 \quad \text{(A2)}$$

The Reuss model, which assumes that the grain boundaries are perpendicular to the stress axis and the stress is uniform from one grain to the next, suggests that the shear modulus, G_R, and the bulk modulus, B_R, are given by

$$G_R = \{[4(s_{11} - s_{12})/5] + (3s_{44}/5)\}^{-1} \quad \text{(A3)}$$

and

$$B_R = [3(s_{11} + 2s_{12})]^{-1} \quad \text{(A4)}$$

Comparison of Equations (A2) and (A4) reveal that both models lead to identical values for the bulk modulus.

An estimate of the upper, G_H, and lower, G_S, bounds for the shear modulus was derived by Hashin and Shtrikman [30, 31], who obtained

$$G_H = G_1 + 3\{[5/(G_2 - G_1) - 4\beta_1]\}^{-1} \quad \text{(A5)}$$

and

$$G_S = G_2 + 2\{[5/(G_1 - G_2) - 6\beta_2]\}^{-1} \quad \text{(A6)}$$

where

$$G_1 = 0.5(c_{11} - c_{12}) \quad \text{(A7)}$$

$$G_2 = c_{44} \quad \text{(A8)}$$

$$\beta_1 = -3(K_V + 2G_1)/[5G_1(3K_V + 4G_1)] \quad \text{(A9)}$$

$$\beta_2 = -3(K_V + 2G_2)/[5G_2(3K_V + 4G_2)] \quad \text{(A10)}$$

Ashby [32] and Frost and Ashby [33] suggested using a geometric mean of Equations (A7) and (A8) since it is related to the elastic energy of a screw dislocation. Thus, the Ashby modulus, G_A, is given by

$$G_A = [0.5\, c_{44}(c_{11} - c_{12})]^{0.5} \quad \text{(A11)}$$

The corresponding Young's modulus, E_i, can be calculated from Equations (A1) – (A3) and (A5) – (A11) using [34]

$$E_i = 9B_V G_i/(3B_V + G_i) \quad \text{(A12)}$$

where G_i is the appropriate shear modulus given by the above models.

A2 Evaluation of the Young's and shear moduli from single crystal data on CaF_2 and LiF

The temperature dependence of c_{11}, c_{12}, c_{44}, s_{11}, s_{12} and s_{44} for CaF_2 and LiF single crystals were compiled from several sources [35–38]. Using Equations A1 to A12, the isotropic elastic moduli were estimated from each set of data as a function of temperature, and the corresponding linear regression equations were obtained. This procedure identified the set of equations required for predicting the upper and lower bounds for the shear and Young's moduli. Fig. A1 and A2 show the variation of the shear modulus with temperature for CaF_2 and LiF, respectively, where it is evident that the experimental data from the different investigations are in excellent agreement with each other. The Ashby and the Reuss models predict the upper and lower bounds, respectively, for CaF_2 (Fig. A1) while the Voigt and the Ashby equations form the upper and lower bounds, respectively, for LiF (Fig. A2). The regression equations for these models are tabulated in Table AI using the data reported by Hart [37] and Vidal [38] for LiF and CaF_2, respectively.

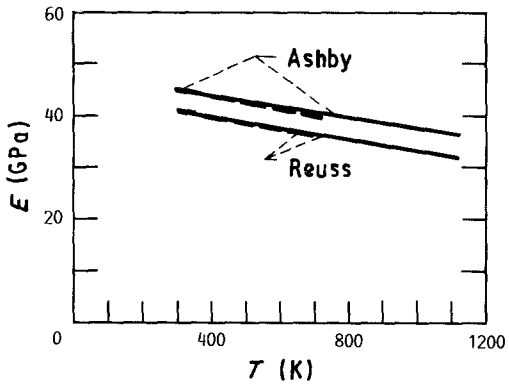

Figure A1 Plots of the isotropic shear modulus against the absolute temperature for data obtained on CaF_2 single crystals [36, 38] showing the upper and lower bounds predicted by the different models (--- [36], —— [38]).

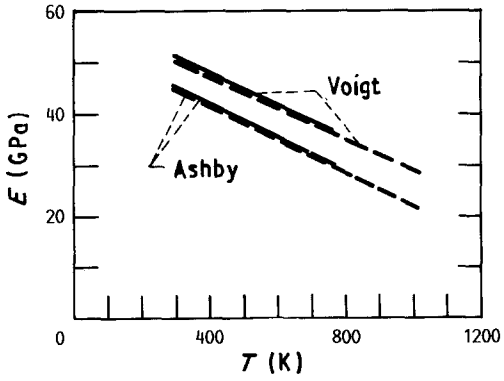

Figure A2 Plots of the isotropic shear modulus against the absolute temperature for data obtained on LiF single crystals [35, 37] showing the upper and lower bounds predicted by the different models (—— [35], --- [37]).

TABLE AI Upper and lower bound regression equations for E and G for CaF_2 and LiF.

Moduli (GPa)	CaF_2[a]		LiF[b]	
	Ashby (upper)	Reuss (lower)	Voigt (upper)	Ashby (lower)
E_i	122.0–0.024T	113.0–0.026T	142.0–0.060T	134.0–0.071T
G_i	47.9–0.010T	44.1–0.011T	59.8–0.031T	54.9–0.033T

Note: [a] Based on the data of Vidal [38].
[b] Based on the data of Hart [37].

A3 Evaluation of the rule of mixtures elastic modulus for the eutectic salt

The upper and lower bound values of E and G were determined for LiF–22% CaF_2 from the sets of equations tabulated in Table AI using the rule of mixtures. Thus,

$$X_{ROM} = V_f X_{fi} + V_m x_{mi} \quad \text{(A13)}$$

where $X_{ROM} = E_{ROM}$ or G_{ROM}, V_f and V_m are the volume fractions of CaF_2 and LiF, respectively, and X_{fi} and X_{mi} are the values of E_i or G_i for CaF_2 and LiF, respectively, calculated from the regression equations tabulated in Table AI.

References

1. A. K. MISRA and J. D. WHITTENBERGER, *Proceedings of the 22nd Intersociety Energy Conversion Engineering Conference (IECEC '87), Philadelphia* (American Institute of Aeronautics and Astronautics, Washington, DC, 1987) p. 188.
2. A. K. MISRA, *J. Electrochem. Soc.* **135** (1988) 850.
3. W. E. ROAKE, *ibid.* **104** (1957) 661.
4. M. O. DUSTIN, J. M. SAVINO, D. E. LACY, R. P. MIGRA, A. L. JUHASZ and C. E. COLES, "Solar Engineering – 1987" edited by D. Y. Goswami, K. Watanabe and H. M. Healey, (The American Society of Mechanical Engineers, New York 1987) p. 574.
5. S. V. RAJ and J. D. WHITTENBERGER, *J. Amer. Ceram. Soc.*, **73** (1990) 403.
6. S. V. RAJ and J. D. WHITTENBERGER, to be published.
7. S. V. RAJ and J. D. WHITTENBERGER, "Strength of Metals and Alloys (ICSMA 8)", edited by P. O. Kettunen, T. K. Lepistö and M. E. Lehtonen (Pergamon, Oxford, 1988). pp. 1007–1012.
8. J. MARX, *Rev. Sci. Instrum.*, **22** (1951) 503.
9. W. H. ROBINSON and A. EDGAR, *IEEE Trans. Sonics Ultrasonics* **SU-21** (1974) 98.
10. J. L. TALLON and A. WOLFENDEN, *J. Phys. Chem. Solids* **40** (1979) 831.
11. M. R. HARMOUCHE and A. WOLFENDEN, *Mater. Sci. Eng.* **84** (1986) 35.
12. J. M. WOLLA and A. WOLFENDEN, ASTM STP 1045 (American Society for Testing and Materials, Philadelphia, 1989) p. 110.
13. "Thermal Expansion (Nonmetallic Solids), Thermophysical Properties of Matter (TPRC Data Series)", Vol. 13, Purdue Research Foundation (Plenum, New York, 1977).
14. W. D. KINGERY, H. K. BOWEN and D. R. UHLMANN, "Introduction to Ceramics" (Wiley, New York, 1976) p. 775.
15. M. E. FINE and N. T. KENNEY, *J. Metals* **4** (1952) 151.
16. M. E. FINE, ASTM STP 129 (American Society for Testing of Materials, Philadelphia, 1952) p. 43.
17. R. W. URE, *J. Chem. Phys.*, **26** (1957) 1363.
18. E. BARSIS and A. TAYLOR, *ibid.* **45** (1966) 1154.
19. Hj. MATZKE, *J. Mater. Sci.* **5** (1970) 831.
20. R. VAN STEENWINKEL, *Z. Naturforsch.* **A29** (1974) 278.
21. A. D. FRANKLIN, *J. Phys. Chem. Solids* **26** (1964) 933.
22. *Idem., ibid* **29** (1968) 823.
23. R. J. LYSIAK and P. P. MAHENDROO, *J. Chem. Phys.* **44** (1966) 4025.
24. G. A. KEIG and R. L. COBLE, *J. Appl. Phys.* **39** (1968) 6090.
25. H. J. STÖCKMANN, D. DUBBERS, M. GRUPP, H. GRUPP, H. ACKERMANN and P. HEITJANS, *Z. Phys.* **B30** (1978) 19.
26. A. G. EVANS and P. L. PRATT, *Phil. Mag.* **20** (1969) 1213.
27. S. CHOWDHURY. S. K. SEN and D. ROY, *Phys. Status Solidi* **B 56** (1973) 403.
28. T. G. STOEBE and R. A. HUGGINS, *J. Mater. Sci.* **1** (1966) 117.
29. G. SIMMONS and H. WANG, "Single Crystal Elastic Constants and Calculated Aggregate Properties: A Handbook" (MIT Press, Cambridge, Mass, 1971).
30. Z. HASHIN and S. SHTRIKMAN, *J. Mech. Phys. Sol.* **10** (1962) 335.
31. *Idem., ibid.* **10** (1962) 343.
32. M. F. ASHBY, *Acta Metall.* **20** (1972) 887.
33. H. J. FROST and M. F. ASHBY, "Deformation-Mechanism Maps: The Plasticity and Creep of Metals and Ceramics" (Pergamon, Oxford, 1982).
34. E. SCHREIBER, O. L. ANDERSON and N. SOGA, "Elastic Constants and Their Measurements" (McGraw-Hill, New York, 1973) p. 6.
35. Y. M. CHERNOV and A. V. STEPANOV, *Sov. Phys.* **3** (1962) 2097.
36. S. P. NIKANOROV, B. K. KARDASHEV and N. S. KAS'KOVICH, *ibid*, **10** (1968) 703.
37. S. HART, *Brit. J. Appl. Phys.* **1** (1968) 1285.
38. D. VIDAL, *C. R. Acad. Sci.* **B279** (1974) 345.

Received 3 October 1989
and accepted 19 March 1990